Arab J Geosci (2013) 6:4981–4991
DOI 10.1007/s12517-012-0806-0

ORIGINAL PAPER

Quaternary coral reefs of the Red Sea coast, Egypt: diagenetic sequence, isotopes and trace metals contamination

Abdelbaset S. El-Sorogy · Hamdy Nour · Emad Essa · Mohamed Tawfik

Received: 9 September 2012 / Accepted: 11 December 2012 / Published online: 28 December 2012

Abstract This study focuses on the diagenetic sequence under marine and meteoric conditions as well as isotopes and trace metals contamination in Quseir and Gebel Zeit areas along the Egyptian Red Sea coast through a series of modern and fossil corals, *Porites lutea* and *Favites pentagona*. The diagenetic sequence begins with deposition of thin fringes of syntaxial aragonite and micritic high-magnesian calcite in the modern corals to completely altered *Porites* and partially altered *Favites* to low-magnesium calcite in the oldest Pleistocene unit. Average $\delta^{18}O$ and $\delta^{13}C$ values of Pleistocene corals in the two studied areas were lower than those of modern corals. Values of modern corals and lower fossil unit indicated coralline limestone, while those of middle and upper fossil units indicated fresh water influences. Average values of trace metals in modern corals were higher than those of Pleistocene counterpart except for Mn. Modern coral samples recorded enrichment in the average values of Pb, Zn, and Mn at Quseir area and enrichment in Co, Cu, and Ni at Gebel Zeit area. This may be attributed mostly to different tourist activities, landfill due to increase urbanization and nearby of Quseir area from the old phosphate harbor at El Hamrawin area, as well as oil exploration and production activities in the Gulf of Suez area. Also, results indicated that most samples of *Porites* have high concentration of trace metals than in *Favites*, especially in Cu, Zn, Mn, and Pb. This may due to high amounts of intergranular porosity and high total surface area of *Porites* in contrast to *Favites*.

Keywords Diagenesis · Isotope analysis · Trace metals · Quaternary · Coral reefs · Red sea coast · Egypt

A. S. El-Sorogy (✉)
Department of Geology and Geophysics, College of Science, King Saud University,
Riyadh, Kingdom of Saudi Arabia
e-mail: asmohamed@ksu.edu.sa

A. S. El-Sorogy · H. Nour · E. Essa · M. Tawfik
Geology Department, Faculty of Science, Zagazig University,
Zagazig, Egypt

Introduction

In their review on the geology of coral reefs in the Red Sea, Behairy et al. (1992) summarized the pressures affected coral reefs are increasing the human activities in the coastal areas, such as, urbanization, industrialization, and growing tourist industry as well as oil spills and untreated sewage from urban areas.

Much of the extensive works on Quaternary reef sequences have been focused on their fossil record, trace and heavy metals, ecology, diagenetic features, and depositional history (James and Ginsburg 1979; Macintyre and Marshall 1988; El-Sorogy 1997a, b; Bastidas and Garcia 1999; Abd El-Wahab and El-Sorogy 2003; Braithwaite and Montaggioni 2009; Gopinath et al. 2009; Kumar et al. 2010; El-Sorogy et al. 2012).

Description of changes in Quaternary sequences are less common and have tended to emphasize the variety of cement matrix present and their relationships to fresh or saline waters or to vadose and phreatic zones (Schroeder 1973; Steinen and Matthews 1973; Dullo 1986; Aıssaoui et al. 1986; Strasser et al. 1992; Melim et al. 2001).

Studies linked between diagenetic sequence of Quaternary coral reefs and their contents of trace metals and oxygen and carbon isotopes along the Red Sea coast are very rare. Therefore, the target of the present work is to study the diagenetic sequence and to document the relationship with trace elements, carbon and oxygen isotope within modern and fossil coral skeletons along the Red Sea coast, Egypt.

Materials and methods

Modern and fossil Pleistocene *Porites lutea* and *Favites pentagona* were sampled from Quseir and Gebel Zeit areas (Fig. 1). Modern coral specimens were collected by scuba diving from 1 to 4 m depth below sea level, from the reef flat to the upper part of the reef slope. For diagenetic alterations, 62 representative samples were chosen for thin sections after impregnation with resin under vacuum. Twenty samples were chosen for SEM examination (Laboratories of National Centre for Research, Egypt and Kiel University, Germany). Twenty-four samples were subsampled for carbon and oxygen isotopes (Erlangen, Germany).

For Zn, Pb, Mn, Fe, Cr, Co, Ni, and Cu analysis, 20 coral samples are washed with sodium hypochloride for 24 h to remove the undesired attached materials and organic tissues (especially for living corals) and then with distilled water. They were oven dried at 60 °C and powdered in an agate mortar; 0.2 g of each sample was digested in 5 ml of HCl and 15 ml HNO_3–$HClO_4$ with ratios 5:1, respectively (Oregioni and Aston 1984). The digested samples were centrifuged at 200 rpm, and the centrifuged liquids were used for the determination of trace elements in modern and fossil coral samples using an inductively coupled plasma atomic emission spectrophotometer (Laboratory of Egyptian Nuclear Material Authority).

Geologic setting

Seismic investigations suggest that reef complex limestones deposited between the Pleistocene and today along the Red Sea coast reach 200 m thick and that these rest on the eroded Pliocene and older deposits (Behairy et al. 1992)

Recent reefs

Recent coral samples were collected from marine area off Wadi Quseir El-Kadium and Gebel Zeit areas (Fig. 1). At Quseir area, the coastal area is wide, while the beach is narrow. The tidal flat is very wide, nearly horizontal, and extends smoothly with very gentle slope seaward. Its bottom floor is rocky, mainly of coralline limestone. The offshore zone includes seagrass and algae on the muddy bottom floor, then fringing reef with high diversity. Field observations proved that, marine area off Wadi Quseir El-Kadium is polluted by different tourist activities and it's nearby from the old phosphate harbor at El Hamrawin area.

At Gebel Zeit area, the tidal fat extends 30–40 m offshore and is followed by a gentle slope to a sandy bottom at 4–5 m deep. Corals are of low diversity than those of Quseir area. Field observations proved that, marine area off Gebel Zeit area is polluted by oil due to its nearby form oil exploration and production activities in the Gulf of Suez area.

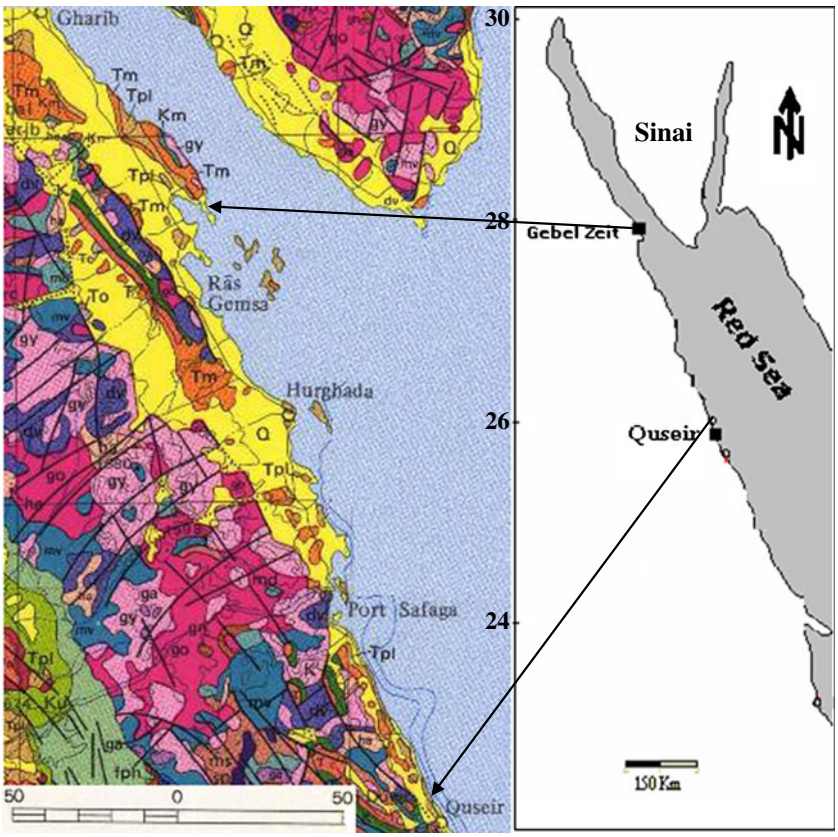

Fig. 1 Location map of the studied sites (after Geologic Map of Egypt 1981). Quaternary ( )—wadi deposits, raised beaches, and coral of the Red Sea coast. Pliocene ( )—marine beds. Miocene ( )—clastics, gypsum, and carbonates. Other symbols are of older rocks

Pleistocene reefs

The Pleistocene raised reefs are one of the most striking features of the coastal plains of the Red Sea coastline (Behairy et al. 1992). These occur in three units with elevations range from 10 to 25 m above the present sea level and with maximum width of about 550 m (El-Sorogy 2008; El-Sorogy et al. 2012). The vertical pattern shows a transgressive sequence in the lower (youngest) and upper (oldest) units and a regressive one in the middle unit. The contact between the different reef units is not always obvious. They form leveled stepped elevations on coastal plain.

In general, the lower unit is easily traced along the Red Sea coast at the two studied areas (Fig. 2a), with width 50 to 120 m. It has three prominent morphological steps at elevations of 1.5, 3.5, and 9 m respectively above the present sea level. The lower unit rests on 0.45 to 1.25 m thick, varicolored conglomeratic layer (surface of nonconformity). The most abundant scleractinians are faviids, poritiids, and acroporids as well as preserved pelecypods, gastropods, and echinoids. It was dated 110,000±8,000 and 141,000–61,000 years BP. at the southern tip of Sinai Peninsula (Gvirtzman and Friedman 1977; Gvirtzman et al. 1992).

The middle unit at the studied areas comprises two morphological terraces of about 8 m thick with elevations of 14 and 19 m above present sea level in the two studied sites. The most abundant fossils (Fig. 2b) are scleractinians, mollusks, and echinoderms. It was dated as 200,000–250,000 years BP at south Sinai Peninsula (Gvirtzman and Friedman 1977) and 205,000 years at the Saudian Red Sea coast (Dullo 1990). Also, Hoang and Taviani (1991) dated 200,000 years to corals at 17 m altitude from Zabarged island.

In Quseir area, the upper unit unconformably overlies the rocks of Pliocene Shagra Formation. The upper unit ranges in elevation from 20 to 25 m above the present sea level. It forms one morphological terrace. The fossils (Fig. 2c) are represented by moderately preserved scleractinians and echinoids. Corals in the same stratigraphic sequence in southern Sinai are dated at 330,000–290,000 years BP by Gvirtzman et al. (1992). The upper unit is absent in Gebel Zeit area, which may be due to erosion or paleorelief topography.

Results

Diagenetic sequence and isotope analysis

For corals, diagenesis refers to the precipitation of secondary aragonite or calcite in skeletal voids or the replacement of skeletal aragonite usually with calcite (Bathrust 1975). During this transformation, isotopes and trace elements are exchanged and removed, thus changing the geochemistry of the coralline matrix which may affect coral proxy records (McGregor and Gagan 2003; Al-Rousan et al. 2007).

The following is a detailed description of the diagenetic sequence within Quaternary modern and fossil coral skeletons and their trace metals and isotope contents in the studied locations.

Modern corals

The first effects of diagenesis occur in a few years in the form of thin fringes of syntaxial aragonite cement developing upon skeletal structures, together with textural changes in the skeleton itself (Perrin and Smith 2007). Micritic high-magnesian calcite and secondary aragonite needles are typical of marine environments (Rabier et al. 2008).

The examined modern corals at the two locations (Figs. 2d, f and 3a–d) mostly show excellent preservation of centers of calcification, in the form of central thin dark line in crossed polarized light with no alteration of the primary microstructure. The radiating fans of the scleroderm-ites are clearly visible (Fig. 3c).

Some thin sections of modern corals show an absence of void filling or marine cement formation (Fig. 2d, e). Such samples may be formed in the recent years. Shinn (1969), recorded growth of aragonite in the modern corals of the Persian Gulf within about 20 years and bulk cementation within ca 400 to 1,000 years. Cavities of other samples contain initials and few ones almost filled with marine cements (Fig. 3b, d).

The most widespread aragonite in modern *Porites* (Fig. 3d) consists of acicular crystals (rods and needles), continuous or irregular linings of subhedral fibrous crystals 30–200 μm long and 2–10 μm wide. It was grown epitaxial on the surfaces of corals or other aragonitic bioclasts, on micrite envelopes and as extensions of crystals forming trabeculae or other structural elements (El-Sorogy 1997a). Stable isotope values of modern corals at Quseir area ranged from 0.10 to 2.00‰ δ^{13}C PDB and from −2.30 to −0.99‰ δ^{18}O PDB for *P. lutea* and ranged from 2.90 to 4.19‰ δ^{13}C PDB and from −2.10 to −0.77‰ δ^{18}O PDB for *F. pentagona*. Isotope values of the two studied species at Gebel Zeit area are located within the values of Quseir area (Fig. 5).

Lower fossil corals

The calcification affecting the aragonitic corals during subaerial diagenesis was generally explained by one of the two following mechanisms (Rabier et al. 2008): first, a partial or full dissolution of the aragonite skeleton, followed by cementation of the primary and secondary voids by an allochthonous low-magnesium calcite (James 1974; Saller 1992). Second, a neomorphism characterized by a concomitant dissolution of the skeletal aragonite and re-precipitation of an autochthonous

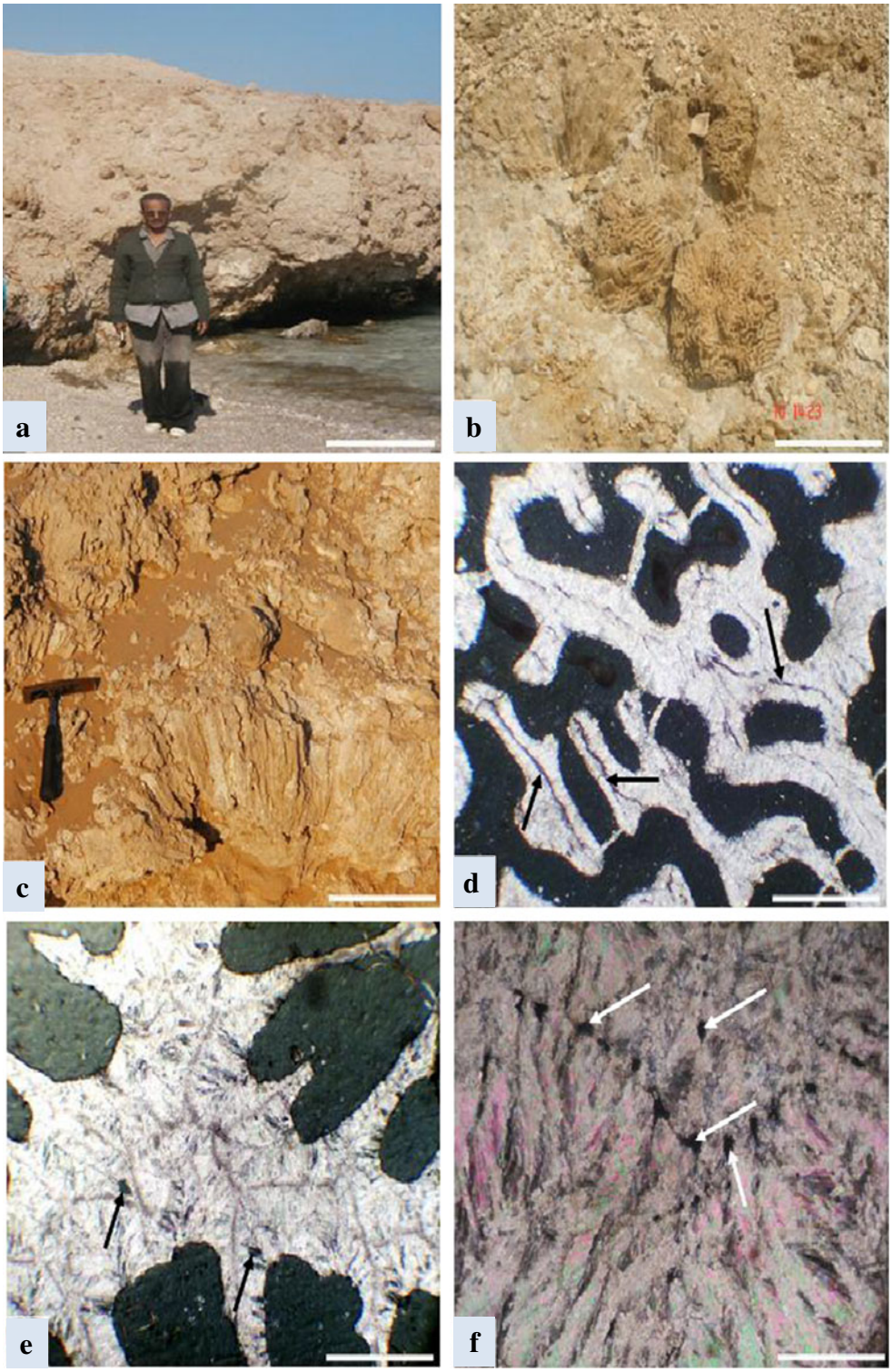

Fig. 2 **a** Lower fossil unit, located just above mean sea level, Quseir area; *bar*=90 cm. **b** Middle fossil unit with large colonies of *Platygyra* in life position, Quseir area; *bar*= 90 cm. **c** Upper fossil unit with large colony of *Porites* in life position, Quseir area; *bar*= 90 cm. **d** Pristine aragonitic *Porites* shows an excellent preservation of centers of calcification (*arrows*) and absence of marine cement (appears in *black*), cross-polarized light of modern corals of Quseir area; *bar*=0.7 mm. **e** Well-preserved wall between three corallites of an aragonitic *Favites* with perforations by micro-bioeroders (*arrows*) and absence of void filling, cross-polarized light of modern corals of Quseir area; *bar*=0.7 mm. **f** Aragonite needles forming the sclerodermites of a well-preserved *Porites* with intra-skeletal porosity (*arrows*), cross-polarized light of modern corals of Quseir area; *bar*=0.4 mm

low-magnesium calcite along a neomorphic front (Maliva and Dickson 1992; Maliva et al. 2000), subsequently followed by the infilling of the primary pores by an allochthonous low-magnesium calcite.

Samples of lower fossil coral unit always display early intraskeletal dissolution zones. These zones characterized by hollow channels along the trabecular axes, a consequence of the centers of the sclerodermites are more likely to be dissolved than any other parts of the skeleton. Leaching is more extensive to the point where calcification centers have been removed, leading to open trabecular centers (Fig. 3e). In this respect, several authors clearly reported

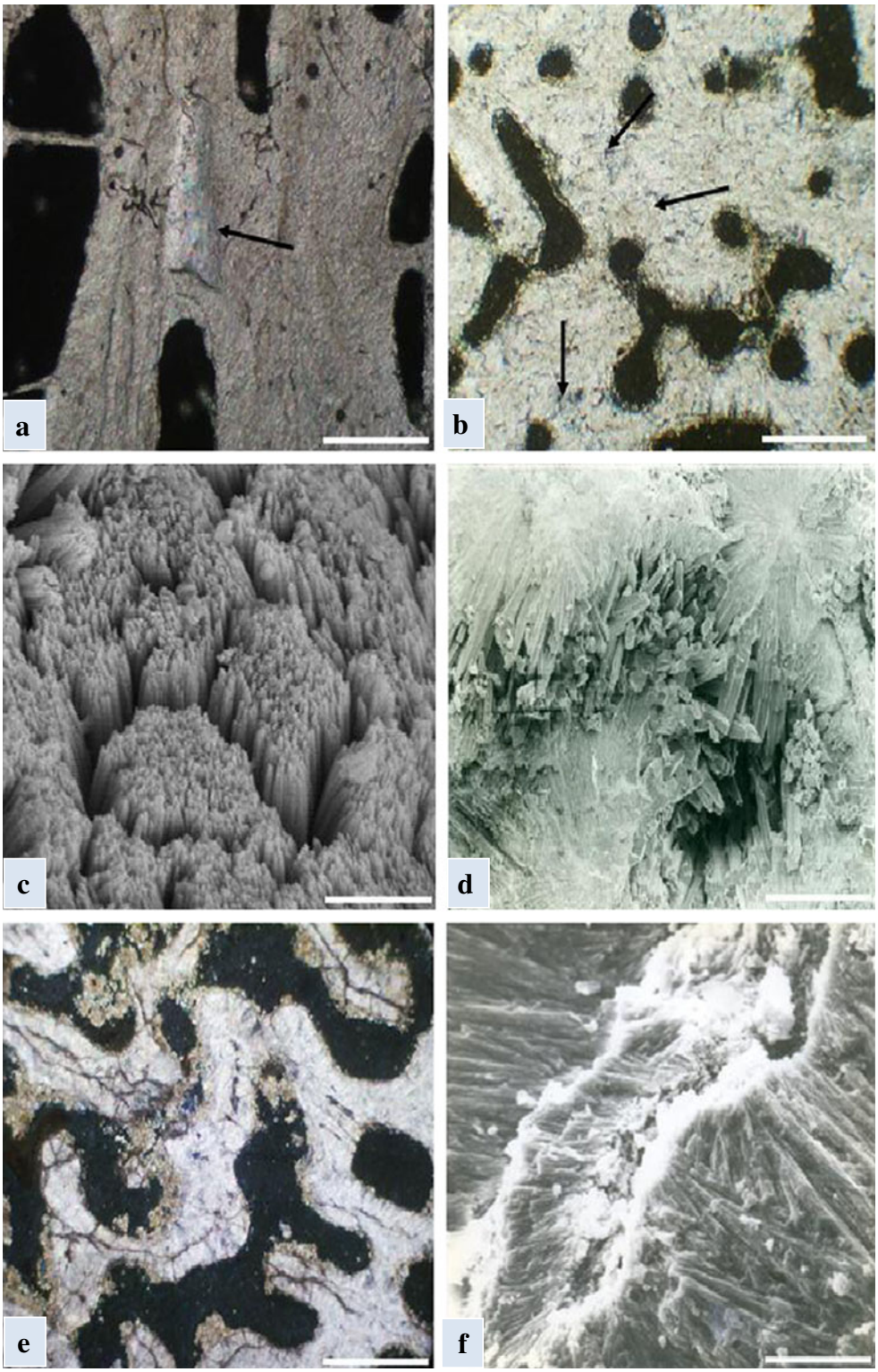

Fig. 3 **a** Marine cements completely fill coral cavity of a pristine aragonitic *Favites* (*arrow*), cross-polarized light of modern corals of Quseir area; *bar*=0.6 mm. **b** Some cavities of *Porites* are completely fill with marine cement (*arrows*) and others with initials, cross-polarized light of modern corals of Quseir area; *bar*=0.6 mm. **c** Aragonite needles forming the sclerodermites of modern *Favites* in Quseir area. Note the intraporosity among sclerodermites, SEM; *bar*=20 μm. **d** Modern *Porites* with marine aragonite cements slightly fill cavities, Gebel Zeit, SEM; *bar*=40 μm. **e** Early intraskeletal dissolution zones along the trabecular axes of *Porites* in Quseir area, lower fossil unit; *bar*=0.7 mm. **f** Typical chalky appearance of trabecular structure of a fossil *Porites* due to meteoric diagenesis, Gebel Zeit, Lower fossil unit; *bar*=20 μm (given by El-Sorogy 2002)

that these centers of calcification favor the flow of leaching water (Gvirtzman and Friedman 1977; Perrin 2003). Next, the water flowing through the central channels can dissolve the tightly packed adjacent aragonite needles, as illustrated by the development of secondary porosity (Fig. 3f), termed chalky zone in the sense of Pingitore (1976).

Chalky aragonite is a dissolution texture often developed in association with precipitation of single crystal calcite (Marshall 1983). This texture is thought to occur in areas saturated with water in dissolution rate greater than calcite precipitation (McGregor and Gagan 2003). Stable isotope values of samples from the lower Pleistocene unit at Quseir

area ranged from −1.10 to 1.37‰ δ^{13}C PDB and from −3.07 to −2.37‰ δ^{18}O PDB for *P. lutea* and ranged from +2.30 to +3.10‰ δ^{13}C PDB and from −3.28 to −2.18‰ δ^{18}O PDB for *F. pentagona*. The values of Gebel Zeit samples of this unit are located within the values Quseir samples (Fig. 5).

Middle fossil corals

Meteoric diagenesis is characterized by the precipitation of low-magnesium calcites (Longman 1980; Rabier et al. 2008). The rate of fresh water flow through the coral skeletons and the length of time it is in contact with the aragonite are variable in accordance with the different kinds of porosity (James and Choquette 1984). Intraskeletal microporosity contains the voids inside the centers of calcification, voids between the aragonite needles of sclerodermites, between adjacent sclerodermites (Figs. 2f and 3c, f), and perforations by micro-bioeroders (Figs. 2e and 3a). The largest size interskeletal macro-porosity is related to interconnected endothecal and fenestral pores (Figs. 2d, f, 3e, and 4c, d, f).

Some samples of middle fossil corals show partial neomorphic alterations, in the form of replacement of aragonite with calcite without destroying the gross coral morphology (Fig. 4a). The neomorphism includes corals, coralline algae, echinoid plates, and some mollusc shells (Fig. 4b). Corals of middle Pleistocene unit from the two studied areas show isotope values range from −2.09 to −0.33‰ δ^{13}C PDB and from −5.46 to −3.04‰ δ^{18}O PDB for *P. lutea* and range from +1.24 to +2.41‰ δ^{13}C PDB and from −6.14 to −4.90 ‰ δ^{18}O PDB for *F. pentagona* (Fig. 5).

Upper fossil corals

Samples of upper (the oldest) fossil corals at Quseir area, show completely altered microstructure, particularly for *Porites* (Fig. 4c, f). Blocky, roughly equant grains are widespread as well as radial groups of crystals of prismatic, obtuse-angled rhombohedral, or nailhead spary calcites mosaic are reprecipitated (Fig. 4c–f).

The equant calcite spars lining or completely fill the primary and secondary voids lead to porosity decreases (Fig. 4e, f). In general, the variations in morphology of calcite cements are interpreted as reflecting changes in water chemistry during crystal growth (Braithwaite and Montaggioni 2009).

In most cases only the micrite envelopes preserve the outline of the original corallites (Fig. 4e). Within skeletons of *F. pentagona*, it is common to find small areas of acicular epitaxial crystals preserved beneath cement overgrowths on neomorphic calcite crystals. These crystals retain distinct optical properties and are not altered and preserved as "ghosts" of the original texture (Fig. 4f). Stable isotope values of samples from the upper (the oldest) Pleistocene unit at Quseir area (Fig. 5) ranged from −2.75 to −1.80‰ δ^{13}C PDB and from −7.16 to −5.44‰ δ^{18}O PDB for *P. lutea* and ranged from −1.55 to −1.34‰ δ^{13}C PDB and from −9.20 to −8.77‰ δ^{18}O PDB for *F. pentagona*.

Trace metals contamination

Pb is a toxic element to corals and is well known as indicator of anthropogenic activities (Beyersmann 1994; El-Sorogy et al. 2012). The average concentration of Pb in recent corals is 21.8 ppm at Quseir area and 19.41 ppm at Gebel Zeit area (Tables 1 and 2). Sample 5 of modern *Porites* at Quseir area has the highest concentration (Table 1). The recorded values are higher than Pb values of the same genera in Gulf of Mannar, India (1.75 ppm) by Kumar et al. (2010) and northwest coast of Venezuela (0.208 ppm) by Bastidas and Garcia (1999). The recorded values of Pb are less than those of Jordanian Gulf of Aqaba (47.91 ppm) by Al-Rousan et al. (2007) and from the Red Sea coast of Saudi Arabia (31 ppm) by Hanna and Muir (1990). The average concentration of Pb in Pleistocene corals is 1.27 ppm at Gebel Zeit area and 0.86 ppm at Quseir area (Tables 1 and 2).

The average concentration of Co in Recent corals is 12.79 ppm at Gebel Zeit area and 11.72 ppm at Quseir area (Tables 1 and 2). In spite of the rarity of Co analysis in worldwide reefs, the recorded Co concentrations are higher than those of Gulf of Mannar, India (2.55 ppm) by Kumar et al. (2010) and Red Sea coast (0.49 ppm) by Abd El-Wahab and El-Sorogy (2003). The average values of Pleistocene samples are 0.38 ppm at Gebel Zeit area and 0.18 ppm at Quseir area (Tables 1 and 2).

The average concentration of Cu in Recent corals is 8.92 ppm at Gebel Zeit area and 6.93 ppm at Quseir area (Tables 1 and 2). Sample 4 of modern *Porites* at Gebel Zeit area has the highest concentrations (Table 2). The recorded Cu values are higher than those of Gulf of Mannar, India (2.4 ppm) by Kumar et al. (2010); Costa Rica (2.0 ppm), Panama (3.8 ppm), and Central America (3.3 ppm) by Guzman and Jimenez (1992); Australia (0.23 ppm) by Esslemont (1996); and Saudi Arabia (1.23 ppm) by Hanna and Muir (1990). They are less than the values of north-west coast of Venezuela (16.33 ppm) by Bastidas and Garcia (1999). In Pleistocene corals, the average concentration of Cu is 0.86 ppm at Gebel Zeit area and 0.76 ppm at Quseir area (Tables 1 and 2).

Zn is an essential micronutrient of coral reefs (Brown and Howard 1985). The average concentration of Zn in Recent corals is 20.81 ppm at Quseir area and 17.50 ppm at Gebel Zeit area, while in Pleistocene samples is 2.86 and 2.74 ppm at Quseir and Gebel Zeit, respectively (Tables 1 and 2). Sample 10 of modern *Favites* at Quseir area has the highest concentration (Table 1). The recorded values of recent samples are mostly higher than all the worldwide reef areas except

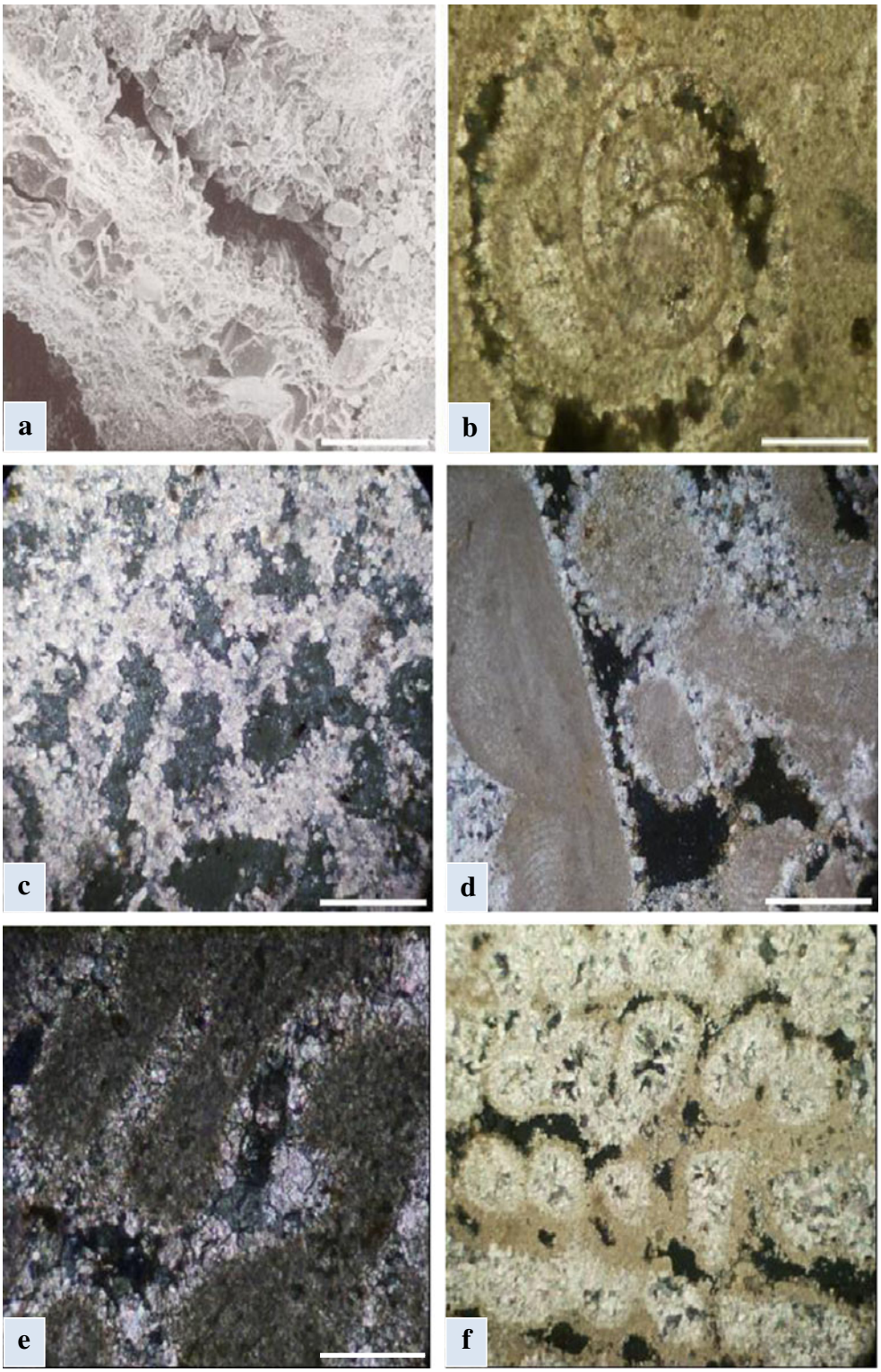

Fig. 4 **a** Partly calcitized fossil *Porites* with deposition of low-magnesium calcite in the primary cavities and in coral cavities, middle fossil corals in Quseir area; *bar*=40 μm. **b** Neomorphism in embryonic gastropod shell, middle fossil corals in Quseir area; *bar*= 0.6 mm. **c** Completely altered *Porites* to low-magnesium calcite (*dog teeth*) by neomorphism and dissolution, Upper fossil corals in Quseir area, bar =0.7 mm. **d** Calcite crystals with rhombohedral "nailhead" terminations among red algal fragments, upper fossil corals in Quseir area; *bar*=0.7 mm. **e** Low-magnesium calcite replaced the former marine cements in the cavities of *Porites*; the original microstructure is completely leached leaving only supporting micrite envelopes, upper fossil corals in Quseir area; *bar*=0.4 mm. **f** Skeletal elements and cements of *Favites* are selectively dissolved and reprecipitated in situ as spary calcite mosaic, upper fossil corals in Quseir area; *bar*=0.4 mm

Gulf of Mannar, India (93.21) by Kumar et al. (2010). The concentration of Zn was 1.87 ppm in Australia (Esslemont 1996), 10.67 ppm in north-west coast of Venezuela (Bastidas and Garcia 1999), 5.52 ppm in Jordanian Gulf of Aqaba (Al-Rousan et al. 2007), and 4.31 ppm from the Red Sea (Abd El-Wahab and El-Sorogy 2003).

Mn concentration in corals is used as indicator of the detrital inputs (Linn et al. 1990). The average concentration of Mn in Recent corals is 9.6 ppm at Quseir area and 6.10 ppm at Gebel Zeit area, while in Pleistocene samples is 21.7 and 18.42 ppm at Quseir and Gebel Zeit, respectively (Tables 1 and 2). Sample 4 of Pleistocene *Porites* in Quseir area

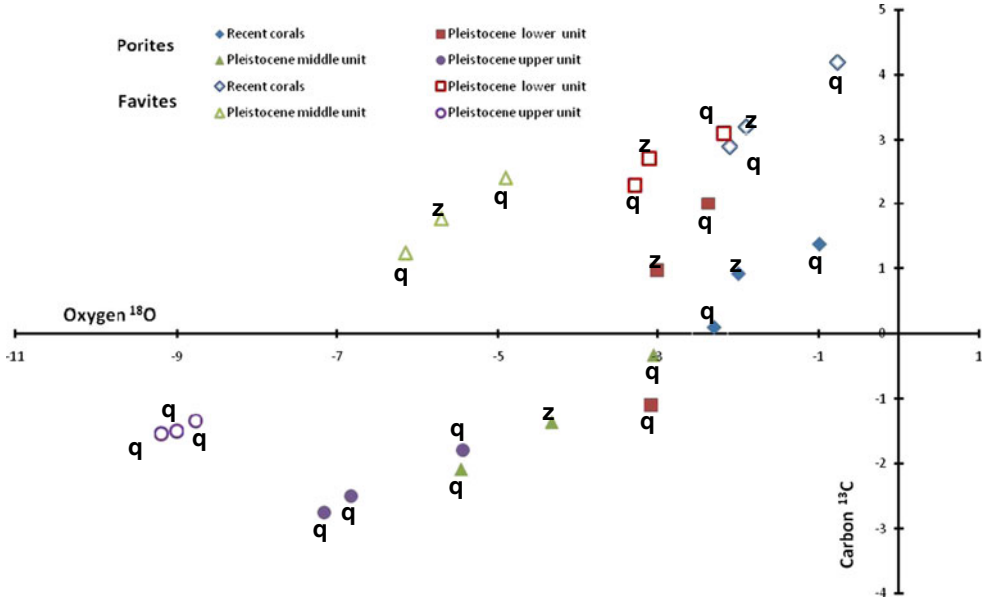

Fig. 5 Cross-plot of stable isotope compositions illustrating overlap of units (*q* Quseir area, *z* Gebel Zeit area)

has the highest concentration (Table 1). As in Zn the concentration of Mn in recent samples are mostly larger than all the worldwide reef areas except Gulf of Mannar, India (118 ppm) by Kumar et al. (2010). The concentration of Mn was 7.3 ppm in Costa Rica (Guzman and Jimenez 1992), 6.62 ppm in Saudi Arabia coast (Hanna and Muir 1990), 8.22 ppm in Jordanian Gulf of Aqaba (Al-Rousan et al. 2007), and 2.07 ppm from the Red Sea (Abd El-Wahab and El-Sorogy 2003).

The average concentration of Ni in recent corals is 19.16 ppm at Gebel Zeit area and 18.8 ppm at Quseir area, while in Pleistocene samples is 0.70 and 0.20 ppm at Gebel Zeit and Quseir, respectively (Tables 1 and 2). Sample 5 of modern *Porites* in Quseir area has the highest concentration (Table 1). The recorded values are higher than those of the Gulf of Mannar, India (0.86 ppm) by Kumar et al. (2010), Australia (1.62 ppm) by Esslemont (1996), and from the Red Sea coast of Saudi Arabia (0.18 ppm) by Hanna and Muir (1990). The average value of Ni in the present recent samples is less than Costa Rica (91.6 ppm), Panama (93.7 ppm), and Central America (93.1 ppm) by Guzman and Jimenez (1992).

Discussion and conclusions

Quaternary coral reefs in Quseir and Gelel Zeit areas along the Red Sea coast are characterized by diagenetic sequence begins with thin fringes of syntaxial aragonite cement and micritic high-magnesian calcite developing upon the skeletal structures.

Table 1 Concentrations of trace metals in Pleistocene and Modern corals at Quseir area

Sample number	Site	Pleistocene						Modern					
		Cu	Ni	Pb	Zn	Mn	Co	Cu	Ni	Pb	Zn	Mn	Co
1	*Porites lutea*	1.21	0.01	0.77	2.89	18.91	0.22	5.5	15.1	20.7	21.1	3.3	11
2		0.83	0.01	1.07	4.49	16.33	0.17	3.1	15.9	21.2	12.1	45	12.4
3		0.54	0.25	0.41	2.93	11.01	0.23	26.3	15.4	17	26.3	4.9	8
4		1.10	0.56	1.39	4.25	70.44	0.05	22.2	18.1	16.4	22.2	5.1	12.1
5		1.13	0.13	0.90	3.55	37.70	0.56	2.9	32	42	30.3	5.6	14.3
6	*Favites pentagona*	0.31	0.57	1.12	2.49	23.97	0.22	1.5	17.8	17.1	9.1	1.8	13
7		0.86	0.09	0.31	3.49	18.70	0.03	2.1	15.7	18	29.7	7	10
8		0.63	0.01	0.91	1.25	2.53	0.06	2.1	16.9	33	14	6.2	14.7
9		0.79	0.34	0.78	2.07	14.91	0.17	1.6	26	18.2	7.3	3.2	12.7
10		0.23	0.05	0.49	1.15	2.52	0.09	2	15.1	14.4	36	13.9	9
Minimum		0.23	0.01	0.31	1.15	2.52	0.03	1.5	15.1	14.4	7.3	1.8	8
Maximum		1.21	0.56	1.39	4.49	70.44	0.56	26.3	32	42	36	45	14.7
Average		0.76	0.20	0.86	2.86	21.70	0.18	6.93	18.8	21.8	20.81	9.6	11.72

Table 2 Concentrations of trace metals in Pleistocene and Modern corals at Gebel Zeit area

Sample number	Site	Pleistocene						Modern					
		Cu	Ni	Pb	Zn	Mn	Co	Cu	Ni	Pb	Zn	Mn	Co
1	*Porites lutea*	1.20	0.99	0.29	1.99	21.81	0.25	8.3	18.1	20.6	13.1	4.0	12.4
2		0.78	0.01	0.99	7.0	15.35	0.11	6.1	17.0	19.2	12.0	4.8	12.9
3		0.50	0.25	2.66	1.45	9.0	0.32	30	19.0	22.0	30.0	5.0	12.3
4		0.10	0.56	2.44	2.01	33.32	0.11	29.2	18.0	19.4	26.3	9.0	13
5		2.15	0.99	1.07	5.32	31.0	0.32	5.1	29	22.3	35.3	3.7	14.9
6	*Favites pentagona*	1.0	0.91	0.34	1.11	19.97	0.19	2.0	15.2	18.3	9.01	2.11	18.0
7		0.49	1.0	1.65	3.0	22.0	0.34	1.9	18.0	12.9	8.02	9.0	13.3
8		0.73	1.34	0.11	0.98	12.22	0.78	2.8	20.1	34.9	22	5.32	14.0
9		0.91	0.91	1.99	1.43	6.56	0.51	2.3	22.8	9.2	4.99	5.0	8.10
10		0.72	0.03	1.19	3.11	13.0	0.83	1.5	14.4	15.3	14.3	13.11	8.98
Minimum		0.10	0.01	0.11	0.98	6.56	0.11	1.5	14.4	9.2	4.99	3.7	8.10
Maximum		2.15	1.34	2.66	7.0	33.32	0.83	30	29	34.9	35.3	13.11	18.0
Average		0.86	0.70	1.27	2.74	18.42	0.38	8.92	19.16	19.41	17.50	6.10	12.79

Samples of lower fossil corals display early intraskeletal dissolution zones along the trabecular axes and precipitation of single crystal calcite. Samples of middle fossil corals show partial neomorphic alterations, in the form of replacement of aragonite with calcite without destroying the gross coral morphology. Upper Pleistocene corals at Quseir area show completely altered microstructure, particularly for *Porites*. Blocky, roughly equant grains are widespread reprecipitated. Skeletons of *Favites* show small areas of aragonitic acicular epitaxial crystals, preserved beneath cement overgrowths on neomorphic calcite crystals.

The difference in diagenetic rate between the two studied species, especially of the upper Pleistocene unit in Quseir area is attributed to the difference in their microstructure and microarchitecture. *P. lutea* consists of small, loosely arranged septa, with isolated trabecular centers, loose crystal packing and high amounts of intergranular porosity (Constantz 1986). These give the skeletons high total surface area for water to flow through. In contract to *F. pentagona*, this is characterized by laminar septa, composed of massive and linear trabecular centers. These centers exhibit tight crystal packing, which restricts the reactive surface area and intercrystalline porosity to a minimum.

There were no significant differences in isotope values between the two studied areas, where isotope values of the coral samples at Gebel Zeit are always located within values of Quseir area (Fig. 5). Marked differences in isotope values are shown among coral units from modern to fossil ones and between the two studied coral species. Stable isotopes of modern corals of the two studied areas are comparable with the values of unit 9 of Braithwaite and Montaggioni (2009) from the Great Barrier Reef. These are consistent with marine sediments and cements (Hudson 1977). Isotopes of lower Pleistocene unit show a marked decrease than modern one, especially in carbon isotopes. These values indicate freshwater signals and mixing zone and are comparable to the data obtained from corals of the youngest Pleistocene terrace of southern Sinai (Strasser et al. 1992) and unit 8 in Great Barrier Reef (Braithwaite and Montaggioni 2009).

Isotope values of *Favites* from middle Pleistocene unit suggest a scatter between limestones with cement derived from the mixing zones, and those reflecting meteoric waters. Isotope values of *Porites* are definitely lighter in carbon than in *Favites*. This difference in isotopes between the two studied species may attribute to the preservation style of the two corals. The negative isotope values of coral samples from upper (the oldest) Pleistocene unit at Quseir area are comparable with the values of unit 7 of Braithwaite and Montaggioni (2009) and with the data obtained from corals of the oldest unit of southern Sinai (Strasser et al. 1992). These indicate a strong fresh water influence (meteoric-derived waters).

The concentration of trace metals in modern coral skeletons is higher than those of Pleistocene counterpart except for Mn (Tables 1 and 2). Average values of Ni, Co, Pb, Cu, and Zn in modern skeletons at Quseir area have nearly 94, 65, 25, 18, and 7 times respectively than those of Pleistocene ones and the average values of Co, Ni, Pb, Cu, and Zn at Gebel Zeit area have 34, 27, 15, 10, and 6 times respectively than those of the Pleistocene ones. Comparison between trace metals analysis of modern skeletons at the two studied areas indicated enrichment in the average values of Pb, Zn, and Mn at Quseir area (Table 1). This may be due to different tourist activities, landfill due to increase urbanization and nearby of Quseir area from the old phosphate harbor at El Hamrawin area, as well as weathering of adjacent rocks. Also average values at Gebel

Zeit area indicated enrichment of Co, Cu, and Ni (Table 2). This may be attributed to oil exploration and production activities in the Gulf of Suez area. Mn values are higher in Pleistocene corals than in modern ones by 3 and 2.3 times at Gebel Zeit and Quseir areas, respectively. This may be attributed to diagenesis process, as during diagenetic transformation, trace elements are exchanged and removed, thus changing the geochemistry of the coralline matrix that may affect coral proxy records (McGregor and Gagan 2003; El-Sorogy et al. 2012).

In comparison with modern worldwide reefs, the recorded values are less than those of Gulf of Aqaba, Jordan, and Red Sea coast of Saudi Arabia (Pb), Gulf of Mannar, India (Zn and Mn), Costa Rica, Panama (Ni), North-west coast of Venezuela (Cu). The recorded values are higher than those of Gulf of Aqaba, Jordan (Zn and Mn), Gulf of Mannar, India (Pb, Co, Cu, and Ni), North-west coast of Venezuela (Pb and Zn), Australia (Cu, Ni, Zn, and Mn), Costa Rica, Panama, Saudi Arabia and Central America (Cu and Mn).

Comparison between trace metal analysis of modern skeletons of the two studied species (Tables 1 and 2), indicated that, most samples of *Porites* have high concentration of trace metals, especially in Cu, Zn, Mn, and Pb than in *Favites*. This perhaps due to high amounts of intergranular porosity and high total surface area for *P. lutea* in contrast to limited surface area and intercrystalline porosity for *Favites*.

Acknowledgment Wish to thank King Saud University, Deanship of Scientific Research, College of Science Research Center for funding the Manuscript. Also the authors are deeply grateful to Prof. Dr. Mohamed Abd El-Wahab, National Institute of Oceanography and fisheries, Red Sea branch, Egypt for collecting modern samples using scuba diving.

References

Abd El-Wahab M, El-Sorogy AS (2003) Scleractinian corals as pollution indicators, Red Sea coast, Egypt. N Jb Geol Paläont Mh 11:641–655, Stuttgart

Aıssaoui DM, Buigues D, Purser BH (1986) Model of reef diagenesis: Mururoa Atoll, French Polynesia. In: Schroeder JH, Purser BH (eds) Reef diagenesis. Springer, Berlin, pp 27–52

Al-Rousan SA, Al-Shloul RN, Al-Horani FA, Abu-Hilal AH (2007) Heavy metal contents in growth bands of *Porites* corals: record of anthropogenic and human developments from the Jordanian Gulf of Aqaba. Mar Pollut Bull 54:1912–1922

Bastidas C, Garcia E (1999) Metal content on the reef coral *Porites* asteroids: an evaluation of river influence and 35 years of chronology. Mar Poll Bull 38:899–907

Bathrust RGC (1975) Carbonate sediments and diagenesis. Elsevier, Amsterdam

Behairy AKA, Sheppard CRC, El-Sayed MK (1992) A review of the geology of coral reefs in the Red Sea. UNEP regional seas reports and studies No. 152, pp. 1–36

Beyersmann D (1994) Interactions in metal carcinogenicity. Toxicol Lett 72:b333–b338

Braithwaite CJR, Montaggioni LF (2009) The Great Barrier Reef: a 700 000 year diagenetic history. Sedimentology 56:1591–1622

Brown BE, Howard S (1985) Responses of coelenterates to trace metals: a field and laboratory evaluation. Proc Fifth Int Coral Reef Congr 6 465–470

Constantz BR (1986) The primary surface area of corals and variations in their susceptibility to diagenesis. In: Schroeder JH, Purser BH (eds) Reef diagenesis. Springer, Berlin, pp 53–76

Dullo WC (1986) Variation in diagenetic sequences: an example from Pleistocene Coral Reefs, Red Sea, Saudi Arabia. In: Schroeder JH, Purser BH (eds) Reef diagenesis. Springer, Berlin, pp 77–90

Dullo WC (1990) Facies, fossil record and age of Pleistocene reefs from the Red Sea (Saudia Arabia). Facies 22:1–40

El-Sorogy AS (1997a) Progressive diagenetic sequence from Pleistocene coral reefs in the area between Quseir and Mersa Alam, Red Sea coast, Egypt. J Geol 41/1:519–540

El-Sorogy AS (1997b) Pleistocene coral reefs of southern Sinai, Egypt: Fossil record, facies analysis and diagenetic alterations. MERC Ain Shams Univ Earth Sci Ser 11:17–36

El-Sorogy AS (2002) Paleontology and depositional environments of the Pleistocene coral reefs of the Gulf of Suez, Egypt. N Jb Geol Paläont Abh 225/3:337–371, Stuttgart

El-Sorogy AS (2008) Contributions to the Pleistocene coral reefs of the Red Sea coast. Egypt Arab Gulf J Sci Res 26(1/2):63–85

El-Sorogy AS, Abd El-Wahab M, Nour HE (2012) Heavy metals contamination of the Quaternary coral reefs, Red Sea coast, Egypt. Environ Earth Sci 67:777–785

Esslemont G (1996) Heavy metals in corals from Heron Island and Darwin Harbour, Australia. Mar Pollut Bull 38(11):1051–1054

Geologic Map of Egypt (1981) The Egyptian geological survey and mining Authority. Scale 1:2000000

Gopinath A, Nair SM, Kumar NC, Jayalakshmi KV, Padmalal D (2009) A base line study of trace metals in a coral reef sedimentary environment Lakshadweep Archipelago. Environ Earth Sci. doi:10.1007/s12665-009-0113-6

Guzman HM, Jimenez CE (1992) Contamination of coral reef by heavy metals along the Caribbean coast of Central America: (Costa Rica and Panama). Mar Pollut Bull 24:554–561

Gvirtzman G, Friedman GM (1977) Sequence of progressive diagenesis in coral reefs. AAPG Stud Geol 4:357–380

Gvirtzman G, Kronfelf J, Buchbinder B (1992) Dated coral reefs of southern Sinai (Red Sea) and their implication to late Quaternary sea levels. Marine Geol 108:29–37

Hanna RG, Muir GL (1990) Red Sea corals as a biomonitors of trace metal pollution. Environ Monit Assess 14:211–222

Hoang CT, Taviani M (1991) Stratigraphic and implications of uranium-series-dated coral reefs from uplifted Red Sea Islands. Quat Res 35:264–663

Hudson JD (1977) Stable isotopes and limestone lithification. J Geol Soc London 133:637–660

James NP (1974) Diagenesis of scleractinian corals in the subaerial vadose environment. J Paleontol 48:785–799

James NP, Choquette PW (1984) Diagenesis of limestones—the meteoric diagenetic environment. Geosci Can 11(4):161–194

James NP, Ginsburg RN (1979) Petrography of limestones from the wall and fore-reef. In: N.P. James and R.N. Ginsburg (eds) The seaward margin of Belize Barrier and Atoll reefs. Int. Assoc. Sedimentol. Spec. Publ. 3:111–152

Kumar KS, Chandrasekar N, Seralathan P (2010) Trace elements contamination in coral reef skeleton, Gulf of Mannar. India Bull Environ Contam Toxicol 84:141–146

Linn LJ, Delaney ML, Druffel ERM (1990) Trace metal in contemporary and seventeenth century Galapagos records of seasonal and annual variations. Geochim Cosmochim Acta 54:387–393

Longman MW (1980) Carbonate diagenetic textures from nearsurface diagenetic environments. AAPG Bull 64:461–487

Macintyre IG, Marshall JF (1988) Submarine lithification in coral reefs: some facts and misconceptions. In: Choat JH, Choat JH, Barnes D, Borowitzka MA, Coll JC, Davies PJ, Flood P, Hatcher BG, Hopley D, Hutchins PA, Kinsey D, Orme GR, Pichon M, Sale PF, Sammarco P, Wallace CC, Wilkinson C, Wolanski E, Bellwood O (eds) Proceedings of the Sixth International Coral Reef Symposium, Townsville, Australia, vol 1. James Cook University Press, Queensland, pp 263–272

Maliva RG, Dickson JAD (1992) The mechanism of skeletal aragonite neomorphism: evidence from neomorphosed mollusks from the upper Purbeck Formation (Late Jurassic–Early Cretaceous), Southern England. Sediment Geol 76:221–232

Maliva RG, Missimer TM, Dickson JAD (2000) Skeletal aragonite neomorphism in Plio-Pleistocene sandy limestones and sandstones. Sediment Geol 136:147–154

Marshall JF (1983) Submarine cementation in a high-energy platform reef: One Tree Reef, southern Great Barrier Reef. J Sed Petrol 53:1133–1149

McGregor HV, Gagan MK (2003) Diagenesis and geochemistry of *Porites* corals from Papua New Guinea: implications for paleoclimate reconstruction. Geochim Cosmochimica Acta 67(12):2147–2156

Melim LA, Swart PK, Maliva RG (2001) Meteoric and marine burial diagenesis. In: R.N. Ginsburg (ed) Subsurface geology of a prograding carbonate margin, Great Bahama Bank: results of the Bahamas drilling project. SEPM Spec. Publ. 70:137–162

Oregioni B, Aston S (1984) The determination of selected trace metals in marine sediments by flameless/flame atomic absorption spectrophotometery. IAEA, Monaco Laboratory (Internal report). (cited from Reference methods on Pollution Studies N. 38, UNEP. 1986)

Perrin C (2003) Diagenèse précoce des biocristaux carbonatés: transformations isominérales de l'aragonite corallienne. Bull Soc Géol Fr 175(2):95–106

Perrin C, Smith DC (2007) Decay of skeletal organic matrices and erarly diagenesis in coral skeletons. Comptes Rendus Paleovol 6:253–260

Pingitore NE (1976) Vadose and phreatic diagenesis: processes, products and their recognition in corals. J Sed Petrol 46:985–1006

Rabier C, Anguy Y, Cabioch G, Genthon P (2008) Characterization of various stages of calcification in *Porites* sp from uplifted reefs—case study from New Caledonia, Vanuatu, Futuna (South–West Pacific). Sediment Geol 211:73–86

Saller AH (1992) Calcitization of aragonite in Pleistocene limestones of Enewetak atoll, Bahamas, and Yucatan—an alternative to thin-film neomorphism. Carbonates Evaporites 7(1):56–73

Schroeder JH (1973) Submarine and vadose cements in Pleistocene Bermuda reef rock. Sediment Geol 10:179–204

Shinn EA (1969) Submarine lithification of Holocene carbonate sediments in the Persian Gulf. Sedimentology 12:109–144

Steinen RP, Matthews RK (1973) Phreatic vs vadose diagenesis: stratigraphy and mineralogy of a cored borehole on Barbados, W.I. J Sed Petrol 43:1012–1020

Strasser A, Chr S, Davaud E, Bach A (1992) Sequential evolution and diagenesis of Pleistocene coral reefs, South Sinai. Egypt Sed Geol 78:59–79